

Unexpected large charge transfer rate mediated by adenine in twisted DNA structure

Yongshun Song¹, Yi Gao^{2,*} and Haiping Fang^{1,3,†}

¹*School of Physics, East China University of Science and Technology, Shanghai 200237, China*

²*Phonon Science Research Center for Carbon Dioxide, Shanghai Advanced Research Institute, Chinese Academy of Sciences, Shanghai 201210, China*

³*School of Physics, Zhejiang University, Hangzhou 310027, China*



(Received 21 June 2023; accepted 15 April 2024; published 24 June 2024)

DNA exhibits remarkable charge transfer ability, which is crucial for its biological functions and potential electronic applications. The charge transfer process in DNA is widely recognized as primarily mediated by guanine, while the contribution of other nucleobases is negligible. Using the tight-binding models in conjunction with first-principles calculations, we investigated the charge transfer behavior of homogeneous GC and AT pairs. We found that the charge transfer rate of adenine significantly changes. With overstretching, the charge transfer rate of adenine can even surpass that of guanine, by as much as five orders of magnitude at a twist angle of around 26° . Further analysis reveals that it is attributed to the turnover of the relative coupling strength between homogeneous GC and AT base pairs, which is caused by the symmetry exchange between the two highest occupied molecular orbitals of base pairs occurring at different twist angles. Given the high degree of flexibility of DNA *in vivo* and *in vitro* conditions, these findings prompt us to reconsider the mechanism of biological functions concerning the charge transfer in DNA molecules and further open the potential of DNA as a biomaterial for electronic applications.

DOI: [10.1103/PhysRevE.109.064412](https://doi.org/10.1103/PhysRevE.109.064412)

I. INTRODUCTION

DNA has been shown to effectively mediate the charge transfer and transport [1–3], which plays a significant role in both biological relevance and many potential electronic applications [4–8]. Since the provocative publication on long-range charge transfer in a DNA assembly by Barton *et al.* [10] the charge transfer and transport process mediated by DNA has been extensively studied for nearly 30 years [9–17]. Particularly, the sequence effects of charge transfer and transport on DNA have attracted intensive interest [18–20], since DNA is comprised of four nucleotide bases: adenine (A), cytosine (C), guanine (G), and thymine (T).

Most of the experimental information on charge transfer and transport in DNA duplex pertains to the transfer of positive charge (electron holes) [21,22]. For the four bases, A^+ , T^+ , and C^+ states were calculated to be 0.44, 1.28, and 1.55 eV higher in energy than G^+ [23]. The lower energy of G^+ makes it a target for oxidation. In addition, experimental measurements of direct electrical conduction on poly(dA)-poly(dT) and poly(dG)-poly(dC) DNA molecules with identical base pairs revealed that the electrical conductivity of poly(dG)-poly(dC) is significantly greater than that of poly(dA)-poly(dT) [24]. When an AT base pair is inserted into the GC chain, the charge transfer efficiency of the G^+ state dramatically reduces [25]. Vice versa, the charge transfer rate in DNA increases dramatically when one AT base pair

in a sequence is replaced with a GC base pair [18]. Besides, *ab initio* calculations also showed that the charge transfer rate between GC pairs is faster than that between AT pairs owing to the stronger electron coupling between GC pairs [26–28], in line with the experimental observations. The charge transfer process in DNA is commonly recognized as mediated by GC pairs, while AT pairs between GC pairs are usually considered as barriers that will reduce charge transfer efficiency [18,22,29–31].

However, some experimental findings contradict these results. For instance, Giese *et al.* [32] discovered that the charge transfer process is not blocked even in A-tracts (i.e., $(dA)_n \cdot (dT)_n$, where $n \geq 4$) [32]. Hole trapping at the A base during charge transfer has also been observed along long A base bridges [33,34]. To explain this phenomenon and the distance-dependent effect of DNA charge transfer, various models have been developed, including superexchange [35], localized hopping [36], and delocalized polaron hopping [24,37,38].

DNA in a living cell is frequently in the situation of structure deformation, such as by thermal fluctuation [39–42] and by DNA bending proteins [43]. Even in crystal structure, the twist angle of DNA is not fixed at the ideal 36° , but rather has a range that is related to the sequence [44]. Extensive studies have investigated these deformations, focusing on single-strand [45] or double-strand DNA [15,41,46]. The deformation achieved either by systematical alterations on the geometrical parameters [46] or by molecular dynamics (MD) simulations [15,41] suggested that the charge transfer between A bases may be also important compared to G bases [15]. However, it is still tacitly accepted that the GC pairs play the dominant role in the charge transfer process in deformed dsDNA.

*Contact author: gaoyi@sari.ac.cn

†Contact author: fanghaiping@sinap.ac.cn

In this work, by using tight-binding models in conjunction with first-principles calculations, we found that the sequence effect of charge transfer in DNA is sensitive to structural torsion. When there is a slight twist from the ideal structure, the charge transfer rate between AT base pairs significantly increases, which can be up to five orders of magnitude faster than that between GC pairs when overstretching. Further frontier orbital analysis revealed that it is attributed to the turnover of the coupling strength between homogeneous GC and AT base pairs upon twisting. The findings challenge the traditional perspective that the charge transfer process in DNA is solely mediated by G^+ and highlights the role of A^+ in the charge transfer process, particularly in cases where twist deformed DNA structure may be present.

II. THEORY OF ELECTRON COUPLING AND CHARGE TRANSFER

Charge transfer and transport along DNA are commonly attributed to coherent superexchange and incoherent hopping. In short distances, coherent superexchange dominates. Therefore, for the dimer system here, we will employ the superexchange theory.

To study the relationship between charge transfer properties and geometric structure, the electronic Hamiltonian can be approximation written in a simple tight-binding models as

$$H = \sum_m e_m \hat{a}_m^+ \hat{a}_m + \sum_{m \neq n} V_{mn} \hat{a}_m^+ \hat{a}_n. \quad (1)$$

Here, \hat{a}_m^+ and \hat{a}_m are the creation and annihilation operators, respectively. e_m is the electron site energy for an electron on molecular site m , and V_{mn} is the electronic coupling matrix element (also known as transfer integral) between site m and site n . Such Hamiltonians have been widely used to compute hole transfer rates [41,45,47]. For simplicity, we only consider a dimer system constituting two homogeneous base pairs, one regarded as the donor and the other as the acceptor. Systems with more than two sites can be approximately deconstructed into this basic process [48].

In one electron approximation, the initial and final states of the charge transfer process in this dimer system are the nonadiabatic highest occupied molecular orbital (HOMOs) of the first excited and ground states of the cationic dimer system, which are mainly contributed by the adiabatic monomer HOMOs ϕ_d and ϕ_a , respectively [47,49]. By utilizing Koopmans' theorem approximation, the energy splitting can be estimated as the difference between the one-electron energies of HOMO and HOMO-1 calculated for the closed-shell neutral dimer. Therefore, HOMO and HOMO-1 in the neutral dimer system are considered as the main factor of the hole transfer process.

In the orthonormal basis of ϕ_d and ϕ_a , the dimer Hamiltonian can be expressed as

$$\mathbf{H} = \begin{pmatrix} e_d & V_{da} \\ V_{ad} & e_a \end{pmatrix}. \quad (2)$$

In the adiabatic basis of ϕ_d and ϕ_a , $e_{d(a)}$ represents the orbital energy of the hole on donor (acceptor) without direct interaction (though the orthonormal transformation will introduce a polarizable effect, as detailed in PS1 of the

Supplemental Material (SM) [50]) between the two monomers. As depicted in Eq. (1), V_{da} represents the electron coupling between donor and acceptor. For homogenous monomers, we have $V_{da} = V_{ad}$.

In the semiclassical Marcus theory [53], the charge transfer rate between two monomers can be calculated by

$$k_{CT} = \frac{2\pi}{\hbar} \frac{|V_{da}|^2}{\sqrt{4\pi\lambda kT}} \exp\left(-\frac{(\Delta E_{12} - \lambda)^2}{4\lambda kT}\right), \quad (3)$$

where V_{da} is the electronic coupling matrix element in Eqs. (1) and (2), and λ is the reorganization energy. ΔE_{12} is the energetic difference between the two eigenstates of nonadiabatic dimer systems, which can be obtained by performing diagonalization on Hamiltonian in Eq. (2). It is expressed as

$$\Delta E_{12} = \sqrt{(e_d - e_a)^2 + (2V_{da})^2}. \quad (4)$$

ΔE_{12} can also be obtained directly as the orbital energy difference between HOMO and HOMO-1 of the dimer systems. More details can be found in the SM [50]. For a complete description of the dynamics of the charge transfer, the kinetic energy due to nuclear motions must be added to Eq. (3), as has been done in a previous study on the mobility of holes in DNA [54]. It has been shown that intramolecular vibration contributes about 0.16 eV to the exponential term in Eq. (3) [55]. This value is smaller than that of λ and falls within the uncertainty range of λ . Some studies have omitted this quantity without significantly affecting the conclusions [45,56].

The reorganization energy λ can be decomposed into inner sphere reorganization energy λ_v and outer sphere reorganization energy λ_s . Inner sphere reorganization energy λ_v takes care of the change in nuclear degrees of freedom, which can be calculated as [56]

$$\lambda_v = E_{\text{cation}}^{\text{neutral}} - E_{\text{cation}}^{\text{cation}} + E_{\text{neutral}}^{\text{cation}} - E_{\text{neutral}}^{\text{neutral}}, \quad (5)$$

where $E_{\text{neutral}}^{\text{neutral}}$ and $E_{\text{cation}}^{\text{cation}}$ are the energies of the neutral and cationic base pair at their optimized structure. $E_{\text{cation}}^{\text{neutral}}$ is the energy of a neutral base pair in cationic state geometry and $E_{\text{neutral}}^{\text{cation}}$ is the energy of a cationic base pair in neutral state geometry. To calculate the terms appearing in Eq. (5), we first optimized the geometry of GC and AT base pairs for both neutral and charged states. Then we carried out single point energy calculations with the optimized geometry for the other charged states.

The outer sphere reorganization energy is the part of the reorganization energy that takes into account the reorganization of the solvent during the charge transfer process. The calculation of outer sphere reorganization energy is very involved and intricate [57,58]. In our calculations, we take the outer sphere reorganization as a parameter, rather than calculating it from the first principles.

The electronic structures of both the monomer (AT and GC) and dimer ([AT], [AT]) and [(GC), (GC)] systems were obtained using DFT level calculations employing program GAUSSIAN16 [59]. In order to demonstrate the accuracy of the calculated results, we conducted computations at various calculation levels, including B3LYP/6-31+G(d), B3LYP/6-311++G(d,p), PW91PW91/Def2TZVP, and PW91PW91/Def2QZVP. The crystal structure data from Arnott [60] is used directly without further geometrical

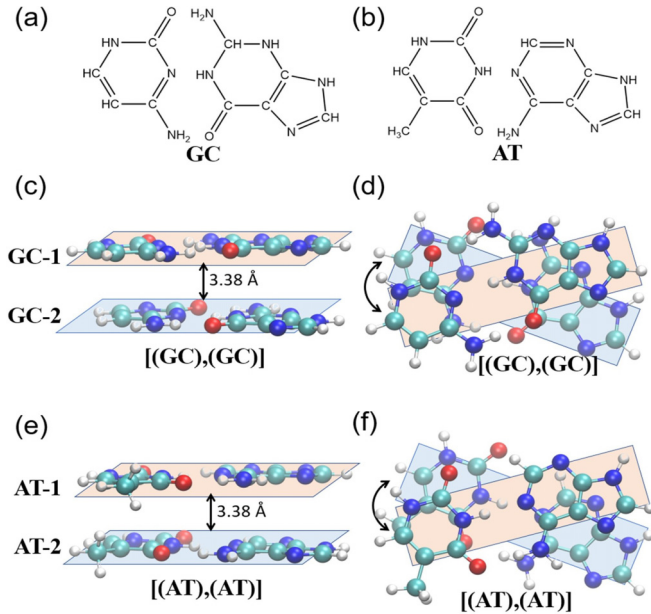


FIG. 1. Chemical structure of (a) GC and (b) AT pair. Side view (c), (e) and bird view (d), (f) of dimers $[(GC),(GC)]$ and $[(AT),(AT)]$. The top and bottom base pairs are denoted as GC-1 (or AT-1) and GC-2 (or AT-2) for $[(GC),(GC)]$ (or $[(AT),(AT)]$), respectively. The elements N, C, O, and H are represented as blue, cyan, red, and white balls, respectively. For $[(GC),(GC)]$, the direction is 5' to 3' for the strand of G from GC-1 to GC-2. For $[(AT),(AT)]$, the direction is 5' to 3' for the strand of A from AT-1 to AT-2.

optimization. The obtained wave functions of the dimer systems are orthogonalized by means of Löwdin's symmetric transformation [52] with the help of CATNIP software [61]. Molecular-orbital plots were generated using the program VMD [62].

III. RESULTS AND DISCUSSION

A. Charge transfer behavior upon twisting

To investigate how the charge transfer behavior of DNA is affected by twist deformation, we began our study on dimers consisting of two stacked base pairs ($[(GC),(GC)]$ and

$[(AT),(AT)]$). The crystal structure data from Arnott [60] was used to build the dimers with the help of the NAB program [63]. The sugar-phosphate backbone was shown to play only a very minor role in the charge transfer process of DNA [64,65] and was omitted in this study. This setup allows us to generate the deformed structure of dimers with any twist angle. The twist angle between the base pairs was adjusted from 21° to 46° with a 1° increment, while keeping the distance along the extension direction of base pairs at 3.38 \AA , as shown in Fig. 1. We recall that, in the ideal B-type DNA, the distance between adjacent base pairs is 3.38 \AA and the twist angle is 36° . The fluctuations and deformation in the base-pair level are not considered in this work.

The charge transfer rate is calculated in the framework of Marcus' theory. As shown in Fig. 2(a), with the increase of the twist angle, the charge transfer rates of $[(GC),(GC)]$ and $[(AT),(AT)]$ both exhibit a pattern of gradually decreasing to a minimum and then increasing in the range $21\text{--}46^\circ$, despite the minima fall at different twist angles (25° for $[(GC),(GC)]$, 38° for $[(AT),(AT)]$). At the ideal twist angle of 36° , the charge transfer rate k_{CT} of $[(GC),(GC)]$ is much higher than that of $[(AT),(AT)]$, which is qualitatively consistent with the previous calculations [36,45] and experimental results. However, when the dimer system deformed in the direction that decreases the twist angle, the charge transfer rate of $[(AT),(AT)]$ becomes larger than that of $[(GC),(GC)]$ after the crossover at the twist angle of about 32° , and the maximum differences reach as high as 10^5 at 25° , which is completely different than the previous conceiving of insensibility of the twist angle [19]. This result indicates that the charge transfer process in DNA would mainly be mediated by the A base when the helical structure of DNA is slightly unwound. We note that the DNA duplex is not very rigid and it is possible to twist more than 10° from its ideal crystal structure [66], and associating with protein will reduce the twist angle most of the time [43,67], which means the charge transfer process via AT can prevail on GC at *in vivo* and *in vitro* conditions.

In the following, we will explain the calculation details and give the scope within which the previous results are valid. First, the electron coupling V_{da} is a key parameter to calculate the value of charge transfer rate. V_{da} is calculated using the method in Sec. II and in PS2 of the SM [50]. The results

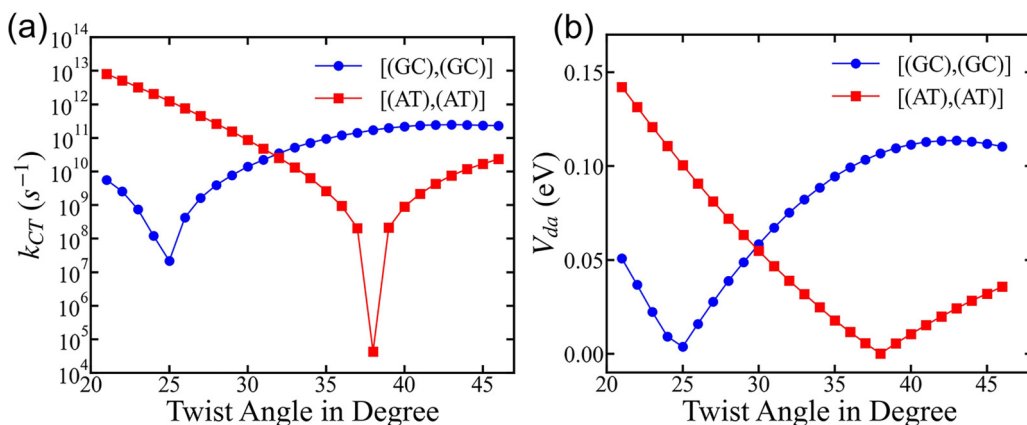


FIG. 2. (a) Charge transfer rates (k_{CT}) of $[(GC),(GC)]$ and $[(AT),(AT)]$ at the twist angle of the range $21\text{--}46^\circ$. (b) Electron coupling matrix elements (V_{da}) of $[(GC),(GC)]$ and $[(AT),(AT)]$ in the range $21\text{--}46^\circ$.

TABLE I. Energies of neutral $E_{\text{neutral}}^{\text{neutral}}$ and cationic $E_{\text{cation}}^{\text{cation}}$ base pairs at their optimized structure, and the energy of a neutral base pair in cationic state geometry $E_{\text{cation}}^{\text{neutral}}$ and energy of a cationic base pair in neutral state geometry $E_{\text{neutral}}^{\text{cation}}$ with unit in Hartree. Inner sphere reorganization energy λ_v (eV) is also shown.

	B3LYP/6-31+G(d)		PW91PW91/Def2QZVP	
	GC	AT	GC	AT
$E_{\text{cation}}^{\text{neutral}}$	-937.555	-921.510	-937.680	-921.620
$E_{\text{neutral}}^{\text{cation}}$	-937.314	-921.237	-937.443	-921.351
$E_{\text{neutral}}^{\text{neutral}}$	-937.302	-921.231	-937.433	-921.347
$E_{\text{neutral}}^{\text{neutral}}$	-937.568	-921.518	-937.693	-921.624
λ_v (eV)	0.70	0.37	0.59	0.20

in Fig. 2(b) were calculated using the B3LYP/6-31+G(d) level of theory; results by other levels of theory are shown in Fig. S1 [50], and they show good consistency. As shown in Fig. 2(b), the electron coupling matrix element V_{da} between [(GC),(GC)] exhibits a minimum at an angle of 25° , while for [(AT),(AT)] the minimal V_{da} falls at 38° . As a result, they cross over at the angle of 31° . Indeed, the crossover behavior of k_{CT} is rooted in the crossover of V_{da} , though the twist angle of the crossover is a bit smaller than that of k_{CT} (about 31° vs 32°). The shift of the twist angle of crossover is originated from the difference in reorganization energy for [(GC),(GC)] and [(AT),(AT)], which will be discussed in detail below.

The reorganization energy is another factor that has a significant impact on the value of k_{CT} . Generally speaking, the reorganization energy λ can be decomposed into inner sphere reorganization energy λ_v and outer sphere reorganization energy λ_s . Using the method mentioned in Sec. II, we calculated the λ_v for GC and AT base pairs. Two different levels of theory were employed to test the validity of the results, which are B3LYP/6-31+G(d) and PW91PW91/Def2QZVP. As shown in Table I, the internal reorganization energies are about 0.70 and 0.37 eV at the B3LYP/6-31+G(d) level of theory, and are about 0.59 and 0.20 eV at the PW91PW91/Def2QZVP level of theory, respectively. The results showed good consistency, and we will use the results of the B3LYP/6-31+G(d) level of theory in the following.

The outer sphere reorganization energy in the literature is varied from 0.2 to even 2 eV [68,69]. In our case, we take the outer sphere reorganization energy as 0.5 eV for both GC and AT base pairs. The different values of reorganization energy were found to only affect the specific value of the charge transfer rate, and did not affect the crossover behavior. As shown in Fig. S2, as the reorganization energy value increases, the charge transfer rate decreases, which is consistent with previous reports [70]. We would like to note that the assumption that the outer sphere reorganization energy is independent of the hopping pairs is crucial for determining the value of the exchange angle. As illustrated in Fig. S2, the exchange angle will shift if the outer sphere reorganization energies of [(GC),(GC)] and [(AT),(AT)] differ.

Since the reorganization energy of [(GC),(GC)] is a little larger than that of [(AT),(AT)], the cross angle will shift to a smaller value with the increase of λ_s . However, within the

range 0.5–1.5 eV, the crossover happens at a very small range, from the twist angle (31° – 32°).

We note that the outer sphere reorganization energy was set to be not changing with the twist angle. A similar treatment has been done in another reference [70]. What is more, compared with DNA stretching, torsion deformation on DNA structure usually has little effect on the rearrangement of surrounding waters. Generally speaking, DNA stretching can enlarge the space between two DNA base pairs, and the water in major groove will be rearranged. For comparison, deformation in twist has no effect on the space between two DNA base pairs, and also has little effect on the width of the major groove, since it is almost kept fixed by the hydrogen bonds between the two bases [71]. Therefore, in our calculations, the outer sphere reorganization energy does not change with the twist angle.

B. Energy difference of nonadiabatic system determines the crossover of charge transfer rate

We have demonstrated that two factors directly influence the behavior of k_{CT} : electron coupling V_{da} and reorganization energy λ . The former determines the crossover behavior of k_{CT} , while the latter affects the absolute value of k_{CT} and causes a shift in the crossover angle. To further investigate the underlying mechanism of the crossover behavior of k_{CT} , we will analyze the reasons behind the crossover behavior of V_{da} . For convenience, we rewrite Eq. (4) as

$$V_{\text{da}} = \frac{1}{2} \sqrt{\Delta E_{12}^2 - (e_d - e_a)^2}. \quad (6)$$

Though the dimers analyzed in this study are constituted of homogeneous monomers, the energy difference $e_d - e_a$ is not zero because the two base pairs are not equivalent [49]. As shown in Figs. 1(c) and 1(d), GC-1 is polarized by GC-2 differently compared to GC-2 polarized by GC-1, and the same for AT-1 and AT-2 shown in Figs. 1(e) and 1(f). The magnitude of energy difference is shown in Fig. S3(a). It can be found that they both show a linear behavior with the increase of twist angle. Though the value for [(AT),(AT)] goes cross the zero line around 25° , it does not account for the minimum in V_{da} along the twist angle. Indeed, the minimum of V_{da} is attributed to the changes in ΔE_{12} . Thus, our subsequent analysis focuses on the changes in ΔE_{12} . As depicted in Fig. S3(b), the minima in the curve of ΔE_{12} are the determining factors for the minimum in the twist angle of V_{da} , which in turn governs the position of the minimum in k_{CT} along the twist angle.

We have noticed that the site energies of the two monomers, and electron coupling were also calculated by Mantela *et al.* based on the Marcus theory, as shown in Figs. 13 and S11 in Ref. [15]. Despite the different methods applied, the values of electron coupling obtained here are very close to theirs, mostly ranging 0.0–0.15 eV [Fig. 2(b) and Fig. S1]. Although the values of site energies (e_d , e_a) of the two monomers differ depending on the DFT level used, the difference ($e_d - e_a$) between the site energies is also very close (for [(GC),(GC)] dimer, Ref. [15]: 0.0–0.2 eV; this work: 0.1–0.2 eV; for [(AT),(AT)] dimer, Ref. [15]: 0.0–0.1 eV; this work: 0–0.05 eV). Thus, our results are reasonably consistent

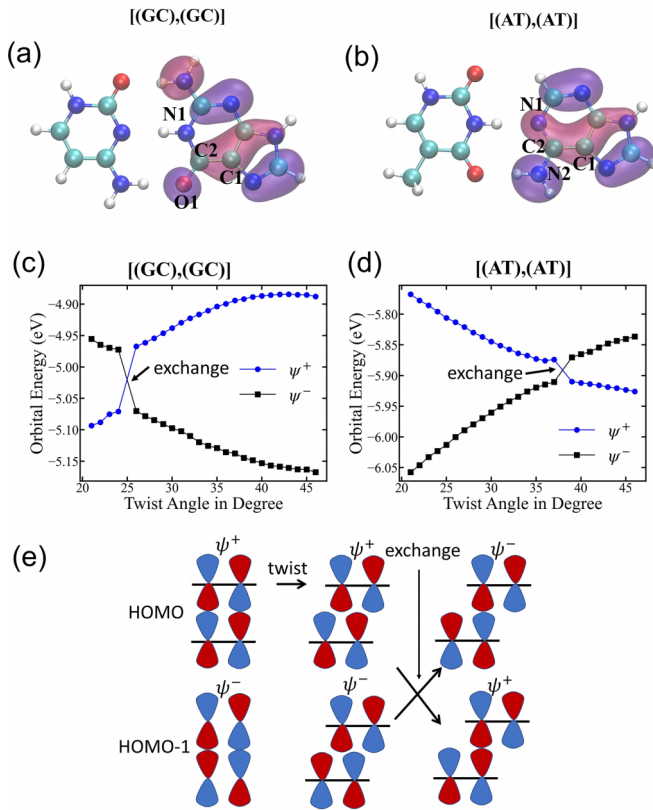


FIG. 3. HOMOs of (a) GC and (b) AT base pairs. The electron is centered on bases G and A, respectively. Orbital energies of the two states ψ^+ and ψ^- for (c) [(GC),(GC)] and (d) [(AT),(AT)] with the twist angle ranging 21–46°. The orbital with the higher energy is the HOMO, and the orbital with the lower energy is the HOMO-1. (e) Cartoon illustrates the exchange of ψ^+ and ψ^- as the twist angle changes.

with the calculations in Ref. [15] for the range of structural adjustments in their molecular dynamics simulations.

In the following, the HOMO and HOMO-1 of [(GC),(GC)] and [(AT),(AT)] were analyzed in detail. As shown in Figs. 3(a) and 3(b), the HOMOs of base pair GC and AT are mainly located on purine bases G and A, respectively. Additionally, there are regions that have different phases (denoted as blue and red) in the single base pair. For the neutral dimer system, their HOMO and HOMO-1 can be formulated as a combination of the HOMOs of two individual base pairs. To clarify, we formulated these two orbitals of the dimer system as ψ^+ and ψ^- , which is

$$\psi^+ = c_{1i}\phi_d + c_{2i}\phi_a,$$

$$\psi^- = c_{1j}\phi_d + c_{2j}\phi_a,$$

where ϕ_d and ϕ_a are the HOMOs of the adiabatic single base pair, and $i, j = 1, 2, i \neq j$. For the elements of the coefficient matrix C , $c_{1i}c_{2i} > 0$, $c_{1j}c_{2j} < 0$. For states ψ^+ and ψ^- , the one having lower orbital energy is the HOMO-1, and the other is the HOMO. The matrix C and wave functions $\psi^{+(-)}$ vary with the twist angles. The energies of these two states are $E(\theta)^+ = \langle \psi^+ | \hat{H} | \psi^+ \rangle$ and $E(\theta)^- = \langle \psi^- | \hat{H} | \psi^- \rangle$, where \hat{H} is the Hamiltonian of the diabatic dimer [see Eq. (1)].

Whether $E(\theta)^-$ is smaller or larger than $E(\theta)^+$ depends on the twist angle.

As shown in Fig. 3(c), with the increase of twist angle from 21° for dimer [(GC),(GC)], the orbital energy of state ψ^+ gradually increases and that of state ψ^- decreases. For twist angles smaller than 25°, state ψ^- is the HOMO due to its higher orbital energy. At the twist angle of 25°, there is a crossover between these two states with the orbital energy of ψ^+ being greater than that of state ψ^- . As a result, state ψ^+ becomes the HOMO. It is similarly demonstrated in Fig. 3(d) for the dimer [(AT),(AT)]. As the twist angle between dimer [(AT),(AT)] increases from 21°, the orbital energy of state ψ^+ gradually decreases, while the orbital energy of state ψ^- increases. At twist angles smaller than 38°, the state ψ^- is the HOMO since it has a larger orbital energy. At the twist angle of 38°, there is a crossover between these two states, and the orbital energy of ψ^- is larger than ψ^+ , making ψ^- the HOMO. At the exchange angle, the energy difference between HOMO and HOMO-1 states is at its lowest. Since the energy difference is the main driving force that promotes the charge transfer process between adjacent base pairs, it is reasonable that the charge transfer rate is also at a minimum at the exchange angle.

To gain a deeper understanding of the interaction between the base pairs, we plotted the isosurface of HOMO and HOMO-1 wave functions in Fig. S5. At the ideal twist angle of 36°, the two well-separated parts of the HOMO of [(GC),(GC)] that are located at the upper and lower base pairs exhibit the same phase, while the two parts of the HOMO of [(AT),(AT)] display opposite phase. This supports the results of Fig. 3, where the HOMO of [(GC),(GC)] is ψ^+ , while the HOMO of [(AT),(AT)] is ψ^- . The exchange of HOMO and HOMO-1 states is further directly illustrated in Figs. S6(a)–S6(d) for [(GC),(GC)] at the twist angles of $\sim 25^\circ$ and in Figs. S6(e)–S6(h) for [(AT),(AT)] at the twist angles of $\sim 38^\circ$, respectively.

C. Structural origin of symmetry exchange

The variation between the exchange angles of [(GC),(GC)] and [(AT),(AT)] originates from the structure difference of bases G and A, where the HOMO of the single base pair is located on. As shown in Figs. 3(a) and 3(b), the presence of $C2 = O1$ in G results in two electrons of the C2 atom participating in the double bond with O1, and the remaining two outermost electrons form simple σ bonds with N1 and C1 respectively. N1 and C2 do not contribute electrons to the π orbital. In the case of base A, C2 forms three σ bonds with N2, C1, and N1 through sp^2 hybridization. The remaining outermost electrons of C2 then would form a π bond with N1, leaving N1 without extra electrons to form an N-H bond with another proton. This results in a different shape of HOMO for single base pairs GC and AT [Figs. 3(a) and 3(b)]. As it is known, the overlap of the same phase leads to a state of lower energy. Thus, the HOMO-1 in the dimer system is arranged in a way that maximizes the overlap of the same phase in the contacted regions of the two HOMOs in a single base pair [as illustrated by the cartoon in Fig. 3(e)]. We noticed that the molecular orbitals contain nodes that separate the positive and negative phase. Upon twisting in the dimer system, the

contact regions between the two orbitals will vary as the twist angle changes gradually. For the HOMO-1 of [(GC),(GC)] (or [(AT),(AT)]), to maximize the overlap of the same phase in the contacted regions in each GC (or AT) base pair, their relative phase will adjust accordingly. As a result, there will be a symmetry exchange between HOMO and HOMO-1 of the dimer when the twist angle changes, and an approximate parabola behavior will appear near the exchange twist angle, as shown in Fig. 2. The electron coupling matrix element V_{da} and corresponding charge transfer rate k_{CT} increase as the twist angle of the two base pairs deviates from the exchange angle. The exchange angles of [(GC),(GC)] and [(AT),(AT)] are 25° and 38° , respectively. Therefore, in the ideal structure with a twist angle of 36° , the electron coupling matrix element V_{da} between [(AT),(AT)] is smaller than [(GC),(GC)], leading to a lower charge transfer rate k_{CT} . However, this trend turns to the opposite for twist angles below 30° .

It should be noted that when other deformations, such as shift and slide, are present, the exchange angle may vary due to structural changes, but the existence of the exchange angle remains certain based on the previous structural analysis.

IV. CONCLUSIONS

In summary, we have theoretically shown that the charge transfer rate of AT pairs significantly increases with a small twist angle deviating from the ideal crystal structure. What is more, it surpasses the charge transfer rate of GC pairs and

can be five orders larger than that of GC when stretching. By performing frontier orbital analysis, we found that there is a turnover of charge transfer rate between AT and GC, which is a consequence of the symmetry exchange at different twist angles. Our work sheds light on the sequence effect of the charge transfer process and provides new ideas to resolve the unusually large charge transfer rate involving AT pairs.

The DNA duplex is very flexible and can easily twist more than 10° from its ideal crystal structure [66], which means the charge transfer process via AT can prevail on GC *in vivo* and *in vitro* conditions. Thus, the traditional view that the charge transfer process in DNA is mainly or even solely mediated by G^+ needs to be reconsidered. The finding here can be further verified by subsequent DNA single-molecule manipulation experiments. We expect to observe a significant increase in DNA conductivity upon twisting the A-rich single-strand DNA. Overall, the effect of AT sequence on the charge transfer of DNA should draw more attention.

ACKNOWLEDGMENTS

We thank Dr. J. Yang, Dr. C. Wang, and Prof. Y. Shao for their constructive suggestions. Support from the Shanghai Science and Technology Innovation Action Plan (Grant No. 23JC1401400), the Fundamental Research Funds for the Central Universities of China, the Guanghe Fund (the second phase), and the Shanghai Supercomputer Center of China are acknowledged.

- [1] D. N. Beratan, *Annu. Rev. Phys. Chem.* **70**, 71 (2019).
- [2] J. D. Slinker, N. B. Muren, S. E. Renfrew, and J. Barton, *Nat. Chem.* **3**, 228 (2011).
- [3] D. Porath, A. Bezryadin, S. de Vries, and C. Dekker, *Nature (London)* **403**, 635 (2000).
- [4] B. Singh, N. S. Sariciftci, J. G. Grote, and F. K. Hopkins, *J. Appl. Phys.* **100**, 024514 (2006).
- [5] W. Shi, S. Han, W. Huang, and J. Yu, *Appl. Phys. Lett.* **106**, 043303 (2015).
- [6] R. G. Endres, D. L. Cox, and R. R. P. Singh, *Rev. Mod. Phys.* **76**, 195 (2004).
- [7] P. Zalar, D. Kamkar, R. Naik, F. Ouchen, J. G. Grote, G. C. Bazan, and T.-Q. Nguyen, *J. Am. Chem. Soc.* **133**, 11010 (2011).
- [8] E. F. Gomez, V. Venkatraman, J. G. Grote, and A. J. Steckl, *Adv. Mater.* **27**, 7552 (2015).
- [9] C. J. Murphy, M. R. Arkin, Y. Jenkins, N. D. Ghatlia, S. H. Bossmann, N. J. Turro, and J. K. Barton, *Science* **262**, 1025 (1993).
- [10] D. B. Hall, R. E. Holmlin, and J. K. Barton, *Nature (London)* **382**, 731 (1996).
- [11] R. P. A. Lima and A. V. Malyshev, *Phys. Rev. E* **106**, 024414 (2022).
- [12] S. Varela, I. Zambrano, B. Berche, V. Mujica, and E. Medina, *Phys. Rev. B* **101**, 241410(R) (2020).
- [13] R. G. Endres, D. L. Cox, R. R. P. Singh, and S. K. Pati, *Phys. Rev. Lett.* **88**, 166601 (2002).
- [14] L. Cong, R. Zhou, Y.-C. Kuo, M. M. Cunniff, and F. Zhang, *Nat. Commun.* **3**, 968 (2012).
- [15] M. Mantela, A. Morphis, K. Lambropoulos, C. Simserides, and R. Di Felice, *J. Phys. Chem. B* **125**, 3986 (2021).
- [16] A. N. Nardi, A. Olivieri, and M. D'Abramo, *J. Phys. Chem. B* **126**, 5017 (2022).
- [17] R. Zhuravel, H. Huang, G. Polycarpou, S. Polydorides, P. Motamarri, L. Katrivas, D. Rotem, J. Sperling, L. A. Zotti, A. B. Kotlyar, J. C. Cuevas, V. Gavini, S. S. Skourtis, and D. Porath, *Nat. Nano.* **15**, 836 (2020).
- [18] E. Meggers, M. E. Michel-Beyerle, and B. Giese, *J. Am. Chem. Soc.* **120**, 12950 (1998).
- [19] T. T. Williams, D. T. Odom, and J. K. Barton, *J. Am. Chem. Soc.* **122**, 9048 (2000).
- [20] K. Kawai, H. Kodera, Y. Osakada, and T. Majima, *Nat. Chem.* **1**, 156 (2009).
- [21] B. Giese, *Acc. Chem. Res.* **33**, 631 (2000).
- [22] F. D. Lewis, R. L. Letsinger, and M. R. Wasielewski, *Acc. Chem. Res.* **34**, 159 (2001).
- [23] A. A. Voityuk, J. Jortner, M. Bixon, and N. Rösch, *Chem. Phys. Lett.* **324**, 430 (2000).
- [24] K. H. Yoo, D. H. Ha, J. O. Lee, J. W. Park, J. Kim, J. J. Kim, H. Y. Lee, T. Kawai, and H. Y. Choi, *Phys. Rev. Lett.* **87**, 198102 (2001).
- [25] F. D. Lewis, T. Wu, X. Liu, R. L. Letsinger, S. R. Greenfield, S. E. Miller, and M. R. Wasielewski, *J. Am. Chem. Soc.* **122**, 2889 (2000).
- [26] A. A. Voityuk, *J. Phys. Chem. B* **113**, 14365 (2009).
- [27] A. A. Voityuk, J. Jortner, M. Bixon, and N. Rösch, *J. Chem. Phys.* **114**, 5614 (2001).
- [28] T. Kubař and M. Elstner, *J. Phys. Chem. B* **112**, 8788 (2008).

- [29] B. Xu, P. Zhang, X. Li, and N. Tao, *Nano Lett.* **4**, 1105 (2004).
- [30] S. R. Patil, V. Chawda, J. Qi, M. P. Anantram, and N. Sinha, *AIP Conf. Proc.* **1953**, 140148 (2018).
- [31] F. D. Lewis, X. Liu, J. Liu, S. E. Miller, R. T. Hayes, and M. R. Wasielewski, *Nature (London)* **406**, 51 (2000).
- [32] B. Giese, J. Amaudrut, A.-K. Köhler, M. Spormann, and S. Wessely, *Nature (London)* **412**, 318 (2001).
- [33] C. Dohno, A. Ogawa, K. Nakatani, and I. Saito, *J. Am. Chem. Soc.* **125**, 10154 (2003).
- [34] K. E. Augustyn, J. C. Genereux, and J. K. Barton, *Angew. Chem. Int. Ed.* **46**, 5731 (2007).
- [35] J. Jortner, M. Bixon, A. A. Voityuk, and N. Rösch, *J. Phys. Chem. A* **106**, 7599 (2002).
- [36] T. Takada, K. Kawai, X. Cai, A. Sugimoto, M. Fujitsuka, and T. Majima, *J. Am. Chem. Soc.* **126**, 1125 (2004).
- [37] M. R. Singh, G. Bart, and M. Zinke-Allmang, *Nanoscale Res. Lett.* **5**, 501 (2010).
- [38] M. R. Singh, *J. Biomater. Sci. Polymer Edition* **15**, 1533 (2004).
- [39] W. Ren, J. Wang, Z. Ma, and H. Guo, *Phys. Rev. B* **72**, 035456 (2005).
- [40] A. A. Voityuk, K. Siriwong, and N. Rösch, *Phys. Chem. Chem. Phys.* **3**, 5421 (2001).
- [41] T. Kubař, P. B. Woiczikowski, G. Cuniberti, and M. Elstner, *J. Phys. Chem. B* **112**, 7937 (2008).
- [42] A. A. Voityuk, K. Siriwong, and N. Rösch, *Angew. Chem. Int. Ed.* **43**, 624 (2004).
- [43] B. Heddi, C. Oguey, C. Lavelle, N. Foloppe, and B. Hartmann, *Nucleic Acids Res.* **38**, 1034 (2009).
- [44] M. A. El Hassan and C. R. Calladine, *Philos. Trans. R. Soc. London Ser. A: Math., Phys. Eng. Sci.* **355**, 43 (1997).
- [45] K. Senthilkumar, F. C. Grozema, C. F. Guerra, F. M. Bickelhaupt, F. D. Lewis, Y. A. Berlin, M. A. Ratner, and L. D. A. Siebbeles, *J. Am. Chem. Soc.* **127**, 14894 (2005).
- [46] S. S. Mallajosyula, A. Gupta, and S. K. Pati, *J. Phys. Chem. A* **113**, 8448 (2009).
- [47] E. F. Valeev, V. Coropceanu, D. A. da Silva Filho, S. Salman, and J.-L. Brédas, *J. Am. Chem. Soc.* **128**, 9882 (2006).
- [48] T. Renger and R. A. Marcus, *J. Phys. Chem. A* **107**, 8404 (2003).
- [49] N. Rösch and A. A. Voityuk, in *Long-Range Charge Transfer in DNA II*, edited by G. B. Schuster (Springer, Berlin, 2004), pp. 37–72.
- [50] See Supplemental Material at <http://link.aps.org/supplemental/10.1103/PhysRevE.109.064412> for details of the calculation methods and additional figures, which includes Refs. [47,49,51,52].
- [51] T. R. Prytkova, I. V. Kurnikov, and D. N. Beratan, *J. Phys. Chem. B* **109**, 1618 (2005).
- [52] P. O. Löwdin, *J. Chem. Phys.* **18**, 365 (1950).
- [53] R. A. Marcus and N. Sutin, *Biochim. Biophys. Acta: Rev. Bioenergetics* **811**, 265 (1985).
- [54] F. C. Grozema, L. D. A. Siebbeles, Y. A. Berlin, and M. A. Ratner, *ChemPhysChem* **3**, 536 (2002).
- [55] M. Bixon and J. Jortner, *Chem. Phys.* **281**, 393 (2002).
- [56] A. Khan, *J. Chem. Phys.* **128**, 075101 (2008).
- [57] V. Rühle, A. Lukyanov, F. May, M. Schrader, T. Vehoff, J. Kirkpatrick, B. Baumeier, and D. Andrienko, *J. Chem. Theory Comput.* **7**, 3335 (2011).
- [58] B. Wang, C. Li, J. Xiangyu, T. Zhu, and J. Z. H. Zhang, *J. Chem. Theory Comput.* **16**, 6513 (2020).
- [59] M. J. Frisch *et al.*, Gaussian, Inc., Wallingford CT, 2016.
- [60] S. Arnott and D. W. L. Hukins, *Biochem. Biophys. Res. Commun.* **47**, 1504 (1972).
- [61] J. S. Brown, [Software] available from https://github.com/JoshuaSBrown/QC_Tools.
- [62] W. Humphrey, A. Dalke, and K. Schulten, *J. Mol. Graphics* **14**, 33 (1996).
- [63] T. J. Macke and D. A. Case, in *Molecular Modeling of Nucleic Acids*, edited by N. B. Leontis and J. SantaLucia, Jr. (American Chemical Society, Washington, DC, 1997), pp. 379–393.
- [64] G. S. M. Tong, I. V. Kurnikov, and D. N. Beratan, *J. Phys. Chem. B* **106**, 2381 (2002).
- [65] S. Priyadarshy, S. M. Risser, and D. N. Beratan, *J. Phys. Chem.* **100**, 17678 (1996).
- [66] S. Kannan, K. Kohlhoff, and M. Zacharias, *Biophys. J.* **91**, 2956 (2006).
- [67] W. K. Olson, A. A. Gorin, X.-J. Lu, L. M. Hock, and V. B. Zhurkin, *Proc. Natl. Acad. Sci. USA* **95**, 11163 (1998).
- [68] J. C. Genereux and J. K. Barton, *Chem. Rev.* **110**, 1642 (2010).
- [69] D. N. LeBard, M. Lilichenko, D. V. Matyushov, Y. A. Berlin, and M. A. Ratner, *J. Phys. Chem. B* **107**, 14509 (2003).
- [70] S. Bag, S. Mogurampelly, W. A. Goddard, III, and P. K. Maiti, *Nanoscale* **8**, 16044 (2016).
- [71] S. Pal, P. K. Maiti, and B. Bagchi, *J. Chem. Phys.* **125**, 234903 (2006).